

Mazzaferro, S., Bermudez, I. and Sine, S. (2016) 'alpha 4 beta 2 Nicotinic Acetylcholine Receptors: Relationships Between Subunit Stoichiometry and Function at the Single Channel Level', *Journal of Biological Chemistry*, 292 (7), pp. 2729-2740.

DOI: <https://doi.org/10.1074/jbc.M116.764183>

This document is the authors' Accepted Manuscript.

License: <https://creativecommons.org/licenses/by-nc-nd/4.0>

Available from RADAR: <https://radar.brookes.ac.uk/radar/items/f3f6c04d-1bef-4700-81f1-058270386a7e/1/>

Copyright © and Moral Rights are retained by the author(s) and/ or other copyright owners unless otherwise waved in a license stated or linked to above. A copy can be downloaded for personal non-commercial research or study, without prior permission or charge. This item cannot be reproduced or quoted extensively from without first obtaining permission in writing from the copyright holder(s). The content must not be changed in any way or sold commercially in any format or medium without the formal permission of the copyright holders.

$\alpha 4\beta 2$ Nicotinic Acetylcholine Receptors: relationships between subunit stoichiometry and function at the single channel level

Simone Mazzaferro¹, Isabel Bermudez⁴ and Steven M. Sine^{1,2,3}

Running title: Single channel properties of $\alpha 4\beta 2$ nAChR

Author affiliations: ¹Receptor Biology Laboratory, Department of Physiology and Biomedical Engineering, ²Department of Neurology, ³Department of Molecular Pharmacology and Experimental Therapeutics, Mayo Clinic College of Medicine, Rochester, MN 55905. ⁴School of Life Sciences, Oxford Brookes University, Oxford OX3 0BP, United Kingdom.

To whom correspondence should be addressed: Steven M. Sine, Department of Physiology and Biomedical Engineering, Mayo Clinic College of Medicine, Rochester, MN 55905, USA. Tel.: +1 507 284 9404, FAX: +1 507 284 9420. E-mail: sine@mayo.edu.

Keywords: nicotinic acetylcholine receptors (AChRs), ligand-gated ion channels, allosteric regulation, Subunit stoichiometry, single channel, conductance, 14-3-3 protein, patch clamp.

ABSTRACT

Acetylcholine receptors (AChRs) comprised of $\alpha 4$ and $\beta 2$ subunits are the most abundant class of nicotinic AChR in the brain. They contribute to cognition, reward, mood and nociception, and are implicated in a range of neurological disorders. Previous measurements of whole-cell macroscopic currents showed that $\alpha 4$ and $\beta 2$ subunits assemble in two predominant pentameric stoichiometries, which differ in their sensitivity to agonists, antagonists and allosteric modulators. Here we compare agonist-elicited single channel currents from receptors assembled with an excess of either the $\alpha 4$ or $\beta 2$ subunit, forming receptor populations biased toward one or the other stoichiometry, with currents from receptors composed of five concatemeric subunits in which the subunit stoichiometry is predetermined. Our results associate each subunit stoichiometry with a unique single channel conductance, mean open channel lifetime and sensitivity to the allosteric potentiator NS-9283. Receptors with the composition $(\alpha 4\beta 2)_2\alpha 4$ exhibit high single channel conductance, brief mean open lifetime and strong potentiation by NS-9283, whereas receptors with the composition $(\alpha 4\beta 2)_2\beta 2$ exhibit low single channel conductance, long mean open lifetime and are not potentiated by NS-9283. Thus single channel current measurements

reveal bases for the distinct functional and pharmacological properties endowed by different stoichiometries of $\alpha 4$ and $\beta 2$ subunits, and establish pentameric concatemers as a means to delineate interactions between subunits that confer these properties.

INTRODUCTION

Nicotinic acetylcholine receptors (AChR) are pentameric ligand-gated ion channels formed from homologous subunits, of which there are many different subtypes (1). The ability to combine different types of subunits into an individual pentamer enables a wide diversity of functional properties and, as a consequence, the ability to meet a range of physiological needs (2). In the brain, the vast majority of ³H-nicotine binding sites arise from AChRs comprised of $\alpha 4$ and $\beta 2$ subunits (3–6). These subunits assemble into pentamers in which the stoichiometry of $\alpha 4$ and $\beta 2$ subunits varies (7, 8). The two predominant subunit stoichiometries differ in their sensitivity to ACh, unitary current amplitude, selectivity for different agonists and antagonists, potentiation by ions or drugs and the agonist concentration dependence of desensitization (8–15). Because the agonist binding sites form at interfaces between the principal face of an $\alpha 4$ subunit and the complementary face of either a $\beta 2$ or $\alpha 4$ subunit, changes in subunit stoichiometry

alter the number of agonist binding sites per pentamer (15, 16). In addition, at interfaces that do not bind agonist, changes in subunit pairing can alter receptor function via allosteric effects (17). Thus understanding the functional consequences of changes in the stoichiometry of $\alpha 4$ and $\beta 2$ subunits is of paramount significance toward the design of drugs to treat nicotine dependence and a variety of neurological and neurodegenerative diseases.

Insight into the relationship between the stoichiometry of $\alpha 4$ and $\beta 2$ subunits and receptor function has been achieved using concatemeric receptors in which five subunits are covalently linked head to tail in a predetermined order and stoichiometry (18). Concatemeric receptors containing two non-consecutive $\alpha 4$ and three $\beta 2$ subunits activate in response to low concentrations of ACh, and mimic the high agonist sensitivity of receptors assembled with an excess of $\beta 2$ over $\alpha 4$ subunits. On the other hand, concatemeric receptors containing three $\alpha 4$ and two non-consecutive $\beta 2$ subunits activate in response to high concentrations of ACh, and mimic the low agonist sensitivity of receptors assembled with an excess of $\alpha 4$ over $\beta 2$ subunits (18). Likewise, the agonist sazetidine-A activates concatemeric receptors containing two non-consecutive $\alpha 4$ and three $\beta 2$ subunits, but not receptors containing three $\alpha 4$ and two non-consecutive $\beta 2$ subunits, in agreement with studies of receptors assembled with an excess of either the $\beta 2$ or $\alpha 4$ subunit, respectively (15, 18, 19). Finally, zinc potentiates agonist-elicited responses of concatemeric receptors containing three $\alpha 4$ and two non-consecutive $\beta 2$ subunits, but not those of receptors containing two non-consecutive $\alpha 4$ and three $\beta 2$ subunits, in agreement with studies of receptors assembled with an excess of either the $\alpha 4$ or $\beta 2$ subunit, respectively (10, 18).

So far, relationships between the stoichiometry of $\alpha 4$ and $\beta 2$ subunits and a receptor's functional properties have been inferred from measurements of agonist-elicited macroscopic currents that yield the average response of the overall receptor population. In addition, functional properties such as unitary conductance, open channel lifetime and kinetics of activation and deactivation are largely inaccessible to macroscopic current recording. Here, using

patch clamp electrophysiology, agonist-elicited single channel currents are recorded from receptors formed in the presence of an excess of either the $\alpha 4$ or $\beta 2$ subunit. These unitary currents are then compared with those from concatemeric receptors in which the stoichiometry and positioning of the subunits is predetermined. The results reveal relationships between the stoichiometry of $\alpha 4$ and $\beta 2$ subunits and functional properties at the level of single receptor channels.

RESULTS

Identification of single channel currents from $\alpha 4\beta 2$ AChRs- Patch clamp recordings, before and after addition of agonist, are required to unambiguously demonstrate single channel currents from $\alpha 4\beta 2$ AChRs. Using an agonist-free recording pipette, a gigaohm seal was established to a BOSC 23 cell transfected with equal amounts of unlinked $\alpha 4$ and $\beta 2$ subunit cDNAs. The baseline current was recorded to verify the absence of single channel currents, and then the membrane-permeable agonist nicotine was added to the extracellular solution (Fig. 1A). After a short delay, single channel openings appeared, initially at a high frequency, followed by a slow decline due to desensitization. Inspection of individual channel openings reveals two distinct unitary current amplitudes of approximately 3 and 4 pA, in agreement with previous studies (9, 20). Applying the same procedure to a BOSC cell transfected with cDNA encoding a pentameric concatemer composed of three non-consecutive $\alpha 4$ and two $\beta 2$ subunits reveals nicotine-activated single channel currents that again decline in frequency due to desensitization (Fig. 1B). Inspection of individual channel openings reveals one unitary current amplitude of approximately 4 pA, in contrast to the dual amplitudes observed with unlinked subunits. These observations establish the identity of agonist-elicited single channel currents from $\alpha 4\beta 2$ AChRs formed by unlinked as well as concatemeric subunits. Furthermore, they suggest unitary current amplitude depends on subunit stoichiometry.

Subunit stoichiometry and single channel current amplitude- To establish that the different unitary current amplitudes arise from receptors

with different subunit stoichiometry, agonist-elicited single channel currents were recorded following transfection of an excess of either the $\alpha 4$ or $\beta 2$ subunit cDNA, as opposed to the equal amounts in Fig. 1A. During receptor assembly, an excess of one subunit over the other is expected to bias the receptor population toward pentamers with an excess of the surplus subunit. To determine subunit stoichiometry, recordings from receptors composed of unlinked subunits were compared with receptors composed of concatemeric subunits containing either two or three $\alpha 4$ subunits plus the pentameric complement of $\beta 2$ subunits. For these determinations, single channel currents were recorded in the cell-attached patch configuration with a concentration of 10 μ M ACh in the recording pipette and a holding potential of -70 mV. Under these conditions, the concentration of ACh exposed to the receptors is held constant, which establishes an equilibrium between activatable and desensitized receptors. When unlinked $\alpha 4$ and $\beta 2$ subunits were transfected in a 1:1 ratio, the single channel current traces, as well as a histogram of single channel current amplitudes, again reveal two distinct current amplitudes of 3.4 and 4.2 pA (Fig. 2A); the histogram is well described by the sum of two Gaussian components. However, when $\alpha 4$ and $\beta 2$ subunits were transfected in a 1:10 ratio, a condition expected to promote assembly of receptors with two rather than three $\alpha 4$ subunits, the single channel traces, as well as the histogram of current amplitudes, reveals one current amplitude of 3.4 pA (Fig. 2B). On the other hand, when the $\alpha 4$ and $\beta 2$ subunits were transfected in a 10:1 ratio, a condition expected to promote assembly of receptors with three rather than two $\alpha 4$ subunits, the single channel current traces and the histogram of current amplitudes reveal one current amplitude of 4.1 pA (Fig. 2C). Thus the unitary current amplitudes obtained from receptors formed with biased ratios of $\alpha 4$ and $\beta 2$ subunits recapitulate those of receptors formed with an equal ratio of the subunits.

Recordings from concatemeric receptors comprised of two non-consecutive $\alpha 4$ subunits and three $\beta 2$ subunits reveal one current amplitude of 3.4 pA (Fig. 2D), in close accord with recordings from receptors formed using a 1:10 ratio of unlinked $\alpha 4$ and $\beta 2$ subunits (Fig. 2B). On

the other hand, recordings from concatemeric receptors comprised of three $\alpha 4$ subunits and two non-consecutive $\beta 2$ subunits reveal one current amplitude of 4.2 pA (Fig. 2E), in close accord with recordings from receptors formed using a 10:1 ratio of unlinked $\alpha 4$ and $\beta 2$ subunits (Fig. 2C). Thus, based on measurements of unitary current amplitude, the subunit stoichiometries inferred for receptors formed using biased ratios of unlinked subunits coincide with the known subunit stoichiometries in concatemeric receptor pentamers.

To quantify the unitary conductance for receptors of each subunit stoichiometry, single channel currents were recorded at different holding potentials, and histograms of single channel current amplitudes were analyzed (Fig. 2F). For each receptor, a plot of the mean current amplitude against holding potential reveals a straight line, the slope of which gives the unitary conductance. Receptors containing two $\alpha 4$ and three $\beta 2$ subunits, whether formed from a 1:10 ratio of unlinked subunits or a concatemeric receptor composed of two non-consecutive $\alpha 4$ and three $\beta 2$ subunits, exhibit a unitary conductance of 48-49 pS. By contrast, receptors containing three $\alpha 4$ and two $\beta 2$ subunits, whether formed from a 10:1 ratio of unlinked subunits or a concatemeric receptor composed of three $\alpha 4$ and two non-consecutive $\beta 2$ subunits, exhibit a unitary conductance of 60 pS. Thus measurements of single channel current amplitude associate a defined stoichiometry and positioning of subunits within the pentamer with a distinct unitary channel conductance.

To confirm the association between unitary current amplitude and subunit stoichiometry, single channel currents elicited by the agonist TC-2559 were recorded in the cell-attached patch configuration at a holding potential of -70 mV (Fig. 2G). TC-2559 was chosen because it is a selective agonist for $\alpha 4\beta 2$ AChRs (21). In all cases the current amplitude from each concatemeric receptor pentamer concurs with that from the corresponding receptors formed from biased ratios of unlinked $\alpha 4$ and $\beta 2$ subunits. Thus, based on recordings with multiple agonists, nicotine, ACh and TC-2559, receptors with greatest unitary conductance correspond to pentamers with three $\alpha 4$ and two non-consecutive

$\beta 2$ subunits, whereas receptors with lowest unitary conductance correspond to receptors with two non-consecutive $\alpha 4$ and three $\beta 2$ subunits.

Subunit stoichiometry and open channel lifetime- To determine whether receptors with different subunit stoichiometry differ in their open channel lifetimes, single channel currents elicited by a concentration of 10 μM ACh were recorded in the cell-attached patch configuration at a holding potential of -70 mV (Fig. 3). The concentration of ACh was designed to minimize ACh-mediated channel block, while still being sufficient to activate receptors with either high or low sensitivity to ACh. Receptors formed with a 1:10 ratio of unlinked $\alpha 4$ to $\beta 2$ subunits exhibit four exponential components of channel openings, with mean durations that differ by approximately one order of magnitude (Fig. 3A; Table 1). The mean duration of the briefest component is approximately 40 μs , while that of the longest component is approximately 10 ms. Analysis of single channel current amplitudes from the same recording reveals one amplitude of approximately 3 pA, verifying that the stoichiometry of these receptors is two $\alpha 4$ and three $\beta 2$ subunits.

Concatemeric receptors comprised of two non-consecutive $\alpha 4$ and three $\beta 2$ subunits also exhibit four exponential components of openings with mean durations similar to those of receptors formed by unlinked subunits (Fig. 3B; Table 1). Previous measurements of macroscopic currents from the same concatemeric receptors reveal an EC_{50} of approximately 1 μM (18), suggesting the ACh concentration of 10 μM ACh used in the single channel recordings approaches full occupancy of the ligand binding sites.

On the other hand, receptors formed with a 10:1 ratio of unlinked $\alpha 4$ to $\beta 2$ subunits exhibit three exponential components of channel openings, with mean durations similar to those of the three briefest components by receptors formed with a 1:10 ratio of subunits. Analysis of single channel current amplitudes from the same recording reveals one amplitude of approximately 4 pA, verifying that the stoichiometry of these receptors is three $\alpha 4$ and two $\beta 2$ subunits. Concatemeric receptors comprised of three $\alpha 4$ and two non-consecutive $\beta 2$ subunits also exhibit three exponential components of openings, although the

mean durations are somewhat longer than those of the corresponding receptors formed by unlinked subunits. Previous measurements of macroscopic currents from these concatemeric receptors reveal an EC_{50} of approximately 100 μM , indicating the ACh concentration of 10 μM in the single channel recordings achieves only partial occupancy of the ligand binding sites. Thus the two different subunit stoichiometries give rise to receptors with distinct distributions of open channel lifetimes in which a component with long mean duration is observed for receptors with two $\alpha 4$ and three $\beta 2$ subunits, whereas receptors with three $\alpha 4$ and two $\beta 2$ subunits lack this component. However, this distinction could arise either from differences in the inherent stability of the open channel or differences in the number of bound agonists.

Subunit stoichiometry and drug potentiation- The drug NS-9283 potentiates $\alpha 4\beta 2$ receptors and is selective for receptors in which the number of $\alpha 4$ subunits is greater than the number of $\beta 2$ subunits. Potentiation arises via a left-shift of the agonist concentration-response relationship rather than an increase of the maximum response. Thus measurements of potentiation of $\alpha 4\beta 2$ receptors by NS-9283 were designed to further distinguish between receptors with different subunit stoichiometry (Fig. 4). A giga-ohm seal was formed to a cell transfected with a 10:1 ratio of $\alpha 4$ to $\beta 2$ subunit cDNAs, and ACh was included in the recording pipette, without or with NS-9283. The ACh concentration of 10 μM is below the EC_{50} for receptors with three $\alpha 4$ and two $\beta 2$ subunits, and the NS-9283 concentration of 10 μM approaches that which maximally potentiate macroscopic currents, and is below that which produces channel block. In the presence of ACh alone, channel openings appear as random isolated events, whereas in the presence of both ACh and NS-9283, channel openings appear in clearly defined clusters of several events in quick succession (Fig. 4A, B). Analyses of single channel current amplitudes from the same recordings revealed one amplitude of approximately 4 pA (data not shown), verifying that the subunit stoichiometry is three $\alpha 4$ and two $\beta 2$ subunits. For recordings in either the absence or presence of NS-9283, histograms of open durations exhibit three exponential components

with similar mean durations for each condition (Fig. 4A, B; Table 2). However, after defining the mean intra-cluster closed duration, histograms of cluster durations comprise three components in the presence of ACh alone, and four components in the presence of ACh and NS-9283 (Fig. 4A, B; Table 3). The mean durations of the two briefest components are similar without and with NS-9283, and likely correspond to channel openings by un-potentiated receptors. Compared to the third component in the presence of ACh alone, the third and fourth components in the presence of NS-9283 are markedly prolonged, and thus correspond to channel openings by potentiated receptors.

Recordings from cells expressing concatemeric receptor pentamers containing three $\alpha 4$ and two non-consecutive $\beta 2$ subunits mirror those from cells expressing receptors formed with an excess of $\alpha 4$ over $\beta 2$ subunits. In particular, channel openings appear as random isolated events in the presence of ACh alone, whereas openings appear in clusters in the presence of ACh and NS-9283 (Fig. 4C, D). Open duration histograms comprise three exponential components of channel openings either without or with NS-9283 (Fig. 4C, D; Table 2). Histograms of cluster durations comprise two components with similar mean durations either without or with NS-9283, thus corresponding to un-potentiated receptors. However a third component, common to both conditions, is prolonged in the presence of NS-9283 compared to that in its absence (Fig. 4C, D; Table 3). Thus NS-9283 potentiates receptors with three $\alpha 4$ and two non-consecutive $\beta 2$ subunits. Furthermore, potentiation by NS-9283 arises through a marked change in channel gating kinetics where channel openings with longest mean duration kinetic coalesce into clusters of events in rapid succession.

To further quantify potentiation by NS-9283, the fraction of channel openings that were followed by a reopening is plotted against the number of reopenings (Fig. 5). A reopening is defined as an opening preceded by a closing shorter than the critical closed time used to define clusters. In the presence of ACh alone, the distribution is well described by a single exponential decay, and the mean number of reopenings, 0.4 to 0.5, is similar whether the receptors are comprised of unlinked or linked subunits. In the presence of ACh and NS-9283, a

second exponential component is observed corresponding to potentiated receptors. For this second component, the mean number of reopenings increases markedly to 3.5 for receptors formed from unlinked subunits, and 9.9 for receptors formed from linked subunits. Thus potentiation by NS-9283 arises from a marked increase in the fraction of channel openings that are followed by a reopening, as well as an increase in the number of reopenings per activation episode

Whether NS-9283 potentiation depends on subunit stoichiometry was evaluated by applying the experimental procedures described in Fig. 4 to cells transfected with either a 1:10 ratio of $\alpha 4$ to $\beta 2$ subunit cDNAs or concatemeric receptor pentamers with two non-consecutive $\alpha 4$ subunits and three $\beta 2$ subunits. For a recording from receptors formed from unlinked subunits, the open duration histogram comprises four exponential components in the presence of ACh alone, while the accompanying closed duration histogram contains two brief and two long duration components (Fig. 6A; Table 2). The two brief closed time components represent infrequent reopening of the same receptor channel, generating a mini-cluster, and the intersection of the second brief with the succeeding long closed time component allows definition of these clusters. The histogram of cluster durations comprises five components, four of which have similar mean durations to those of the open duration histogram, which thus represent distinct kinetic classes of isolated channel openings, while the fifth component represents successive openings of the same channel (Table 3). For a recording obtained in the presence of both ACh and NS-9283, the open duration histogram comprises four exponential components, and the accompanying closed duration histogram contains two brief and two long duration components (Fig. 6B; Table 2). The cluster duration histogram comprises three exponential components, the means of which are briefer, rather than longer, than those in the absence of NS-9283, indicating lack of potentiation by NS-9283, and possibly block of the channel (Table 3). Single channel data from concatemeric receptor pentamers containing three non-consecutive $\beta 2$ and two $\alpha 4$ subunits mirror those from receptors formed from biased ratios of unlinked subunits, showing briefer rather than

longer channel openings in the presence of NS-9283 (Fig. 6C, D; Tables 2, 3). Thus NS-9283 does not potentiate receptors with two $\alpha 4$ and three $\beta 2$ subunits, and is selective for receptors with three $\alpha 4$ and two $\beta 2$ subunits.

DISCUSSION

Previous work, based on measurements of agonist-elicited macroscopic currents, established that $\alpha 4$ and $\beta 2$ subunits assemble with variable subunit stoichiometry producing at least two populations of receptor pentamers (7–9). Evidence included a biphasic agonist concentration-response relationship in which the magnitudes of the high and low affinity components varied, depending on the ratios of either the mRNA or cDNA encoding the two subunits. Furthermore, analyses of purified cell-surface receptors showed that the molar ratio of $\alpha 4$ to $\beta 2$ subunits depended on the ratio of the mRNAs encoding the two subunits (9). Studies of pentameric concatemers, in which the stoichiometry and positioning of subunits is predetermined, confirmed that agonist sensitivity depended on the stoichiometric ratio of the $\alpha 4$ and $\beta 2$ subunits, and identified two constructs that recapitulated the high and low agonist sensitivities of receptors formed from unlinked subunits (15, 18). The present results, based on agonist-elicited single channel currents, establish that receptors with different subunit stoichiometry differ in their unitary current amplitudes, kinetics of channel closing, and susceptibility to drug potentiation, as summarized in Table 4. The overall results provide evidence for independent as well interdependent subunit contributions to receptor function and pharmacology.

Previous single channel recordings from receptors comprised of $\alpha 4$ and $\beta 2$ subunits showed multiple unitary current amplitudes, in accord with multiple receptor populations (9, 22, 23). Recently, a study of receptors assembled from biased ratios of unlinked subunits revealed either uniformly high or low unitary conductance depending on which subunit was present in excess (20). However, the question of subunit stoichiometry remained. Herein, by comparing receptors formed from biased ratios of unlinked subunits with receptors formed from concatemeric subunits, we associate a defined subunit stoichiometry and positioning with a particular

unitary conductance; receptors with two non-consecutive $\alpha 4$ and three $\beta 2$ subunits exhibit a conductance of 48 pS, whereas receptors with two non-consecutive $\beta 2$ and three $\alpha 4$ subunits exhibit a conductance of 60 pS (Table 4). The conductance differences likely originate from differences in charged residues in the extracellular ring that borders the second transmembrane domain (M2) where the $\beta 2$ subunit contains a lysine residue and the $\alpha 4$ subunit contains a glutamate (24). The recent crystal structure of the human $(\alpha 4\beta 2)_2\beta 2$ receptor revealed that these residues project into the path of ion flow at the entrance to the pore domain (31). Previous studies showed that these two residues confer differences in calcium permeability between receptors with different stoichiometric ratios of $\alpha 4$ and $\beta 2$ subunits (12). However the present studies were done in the absence of calcium, so the conductance difference arises from differences in permeability of monovalent alkali ions. The residues in the inner and intermediate rings of charge, between M1 and M2 at the cytoplasmic side of the membrane, are negatively charged in both the $\alpha 4$ and $\beta 2$ subunits (24). Thus, as concluded in classical work that unveiled three rings of charge that contribute to ion conductance, the $\alpha 4$ and $\beta 2$ subunits likely contribute independently of each other according to the sign of the charge in their extracellular ring (25).

Our studies show that receptors with different stoichiometric compositions of subunits differ in their distributions of open channel durations. This observation is significant because each type of receptor contains two ligand binding sites formed at interfaces between $\alpha 4$ and $\beta 2$ subunits, and occupancy of these sites is coupled to channel opening. Furthermore an ACh concentration of 10 μ M is sufficient to occupy both binding sites on receptors in which the fifth subunit is $\beta 2$, as these receptors are highly sensitive to ACh. However, when the fifth subunit is $\alpha 4$, a third ligand binding site forms at the interface between $\alpha 4$ and $\alpha 4$ subunits, and the resulting receptors exhibit relatively brief channel openings, as shown by the absence of an exponential component of openings with long mean duration. Thus the presence of an $\alpha 4$ - $\alpha 4$ ligand binding site has an apparent allosteric effect on the $\alpha 4$ - $\beta 2$ ligand binding sites, either reducing

their affinity for ACh or reducing the ability of the channel to open in response to occupancy by ACh. This allosteric effect could originate from a change in symmetry of the $\alpha 4\text{-}\beta 2$ binding sites. In particular, for high sensitivity, low conductance receptors, the subunits that form one $\alpha 4\text{-}\beta 2$ site are flanked by $\beta 2$ and $\alpha 4$ subunits, while those that form the other site are flanked by $\beta 2$ and $\beta 2$ subunits (Table 4). On the other hand, for low sensitivity, high conductance receptors, the subunits that form one $\alpha 4\text{-}\beta 2$ site are flanked by $\beta 2$ and $\alpha 4$ subunits, while those that form the other site are flanked by $\alpha 4$ and $\alpha 4$ subunits.

Of further importance is our observation that receptors with both stoichiometric compositions of subunits exhibit multiple exponential components of channel openings: four components for high sensitivity, low conductance receptors, and three components for low sensitivity, high conductance receptors. Assuming that the $\alpha 4\text{-}\beta 2$ binding sites are non-equivalent, owing to asymmetry in their neighboring subunits, for high sensitivity, low conductance receptors, three components could arise from two species of singly occupied receptors and one component from the doubly occupied receptor (Table 4). However, four components are observed, suggesting openings may arise from a closed state intermediate between the resting and open channel states (26, 27). For low sensitivity, high conductance receptors, the three observed exponential components could arise from three species of singly occupied receptors, which is plausible given that the agonist concentration is low. With higher concentrations of agonist, additional exponential components are expected due to doubly and triply occupied receptors. Further insights into kinetic mechanism could thus emerge from studies of the distribution of channel open times as a function of agonist concentration.

Previous studies demonstrated that the drug NS-9283 potentiates receptors with an excess of $\alpha 4$ over $\beta 2$ subunits but not receptors with an excess of $\beta 2$ over $\alpha 4$ subunits (11). Our findings confirm that potentiation depends on subunit stoichiometry, but moreover, they define the stoichiometry and positioning of subunits that confer potentiation, and reveal the kinetic basis for potentiation. In the absence of NS-9283, individual channel openings appear predominantly

in isolation, and the number of reopenings per activation episode follows a single exponential decay. However, in the presence of the drug, a second exponential component is observed comprised of clusters of closely spaced events. This change in kinetics is reminiscent of the clustering of channel openings that occurs as the concentration of agonist is increased (28). Thus although NS-9283 does not elicit channel opening by itself, when it is present together with a low concentration of agonist, the kinetics of channel opening resemble those at high concentrations of agonist. It is possible that NS-9283 acts as a co-agonist of ACh by binding to the $\alpha 4\text{-}\alpha 4$ binding site, while ACh binds to the two $\alpha 4\text{-}\beta 2$ sites (29). However, the site for NS-9283 binding could be elsewhere, such as the $\beta 2\text{-}\alpha 4$ interface, which does not bind agonist. In this scenario, agonist would bind to three sites, two $\alpha 4\text{-}\beta 2$ and the $\alpha 4\text{-}\alpha 4$, while the drug binds to one or both $\beta 2\text{-}\alpha 4$ interfaces. Alternatively, NS-9283 may bind at a non-subunit interface, while the agonist binds to the three ligand binding sites. Future studies with concatemeric receptors could potentially distinguish between these mechanisms.

Our findings not only identify three functional attributes of $\alpha 4\beta 2$ receptors that depend on subunit stoichiometry, but they also identify a positioning of subunits within the pentamer that confers these attributes (Table 4). In particular, in both stoichiometric arrangements, one pair of $\alpha 4$ subunits is separated by a $\beta 2$ subunit, as opposed to being consecutive. This non-consecutive arrangement of $\alpha 4$ subunits is reminiscent of the *Torpedo* AChR in which the two $\alpha 1$ subunits are non-consecutive (30), and is identical to that in the crystal structure of the $(\alpha 4\beta 2)_2\beta 2$ receptor (31).

Our findings establish concatemeric pentamers combined with single channel measurements as a means to clarify mechanisms of activation and potentiation of $\alpha 4\beta 2$ receptors. By subunit-selective mutagenesis, one could determine whether agonist occupancy of the $\alpha 4\text{-}\alpha 4$ site alone is responsible for the kinetic differences between receptors with the two stoichiometric compositions of subunits, or whether the presence of a third $\alpha 4$ subunit is responsible. Analogously, one could determine whether potentiation by NS-9283 is mediated by a co-agonist mechanism in which the drug binds to

the $\alpha 4$ - $\alpha 4$ site, or whether potentiation arises through binding to non-canonical $\beta 2$ - $\alpha 4$ sites or a site distinct from subunit interfaces. Both investigations require single channel measurements as a functional endpoint. Finally, our findings offer a means to clarify mechanisms of disease causing mutations of $\alpha 4\beta 2$ receptors by determining whether the functional consequences of the mutations depend on subunit stoichiometry.

EXPERIMENTAL PROCEDURES

Expression of unlinked and linked human $\alpha 4\beta 2$ nAChRs- cDNAs encoding unlinked $\alpha 4$ and $\beta 2$ subunits, $(\alpha 4\beta 2)_2\alpha 4$ and $(\alpha 4\beta 2)_2\beta 2$ concatemeric subunits, and the chaperone protein 14-3-3 were individually sub-cloned into a modified pCI mammalian expression vector (Promega), as previously described (15, 18). The 14-3-3 chaperone increases expression of $\alpha 4\beta 2$ nAChRs formed by unlinked as well as concatemeric subunits (18, 32). BOSC 23 cells, a cell line derived from HEK 293 cells (33), were maintained in Dulbecco's modified Eagle's medium (DMEM, Gibco) with 10% fetal bovine serum, and transfected by calcium phosphate precipitation, as previously described (34–36). For experiments with receptors formed from unlinked subunits, three different ratios of $\alpha 4$, $\beta 2$ and 14-3-3 cDNAs were used: 1:1:1, 10:1:1 and 1:10:1. Varying the ratio of $\alpha 4$ to $\beta 2$ subunit cDNAs biases the receptor population toward a single subunit stoichiometry in both mammalian cell lines (9) and *Xenopus laevis* oocytes (8). The amounts of $\alpha 4$ and $\beta 2$ cDNAs ranged from 0.3 to 3 μg for each 35 mm culture dish of cells. Transfections were carried out for 4 to 16 hours, followed by medium exchange. Single channel recordings were made 48-72 hours post transfection. For experiments with receptors formed from concatenated subunits, $(\alpha 4\beta 2)_2\alpha 4$ and $(\alpha 4\beta 2)_2\beta 2$, the total amount of concatemer cDNA was 1-10 μg per 35 mm culture dish. Furthermore, following transfection at 37°C, the cells were incubated at 30°C until use, which increases expression of receptors on the cell surface (37). Single channel recordings from cells expressing concatenated receptors were made 72 to 96 hours post transfection.

Drugs- Acetylcholine (ACh) was purchased from Sigma-Aldrich (St Louis, MO,

USA); 4-(5-ethoxy-3-pyridinyl)-*N*-methyl-(3*E*)-3-buten-1-amine difumarate (TC-2559) and 3-[3-(3-Pyridinyl)-1,2,4-oxadiazol-5-yl]benzotrile (NS-9283) were purchased from Tocris (UK).

Patch clamp recordings- Single-channel recordings were obtained in the cell-attached patch configuration (38) at a membrane potential of -70 mV and a temperature of 20°C, as previously described (39, 40). For all experiments, the extracellular bathing solution contained (mM): 142 KCl, 5.4 NaCl, 1.8 CaCl₂, 1.7 MgCl₂, and 10 HEPES, adjusted to pH 7.4 with NaOH. The pipette solution contained (mM): 80 KF, 20 KCl, 40 K-aspartate, 2 MgCl₂, 1 EGTA, 10 HEPES, adjusted to pH 7.4 with KOH (41, 42). Concentrated stock solutions of ACh and TC-2559 were made in pipette solution and stored at -80°C until the day of each experiment. A concentrated stock solution of NS-9283 was prepared in DMSO, stored at -80°C , and added to the pipette solution the day of each experiment. Pipette solution without NS-9283 contained an equivalent volume of DMSO to achieve a final concentration of 0.2% (v/v). Patch pipettes were pulled from glass capillary tubes (No.7052, Garner Glass) and coated with Sylgard (Dow Corning).

For experiments in which nicotine was applied to the extracellular bathing solution, a giga-ohm seal was initially established to a cell using a patch pipette filled with agonist-free pipette solution. A baseline current was recorded for 1-5 minutes, and then nicotine was added drop wise to the extracellular solution to establish a final extracellular concentration of 342.5 μM . Continuous recordings were obtained before, during and after nicotine addition.

Data Analysis- Single-channel currents were recorded using an Axopatch 200B patch-clamp amplifier (Molecular Devices), with the gain set at 100 mV/pA and the internal Bessel filter at 10 kHz. Currents were sampled at intervals of 20 μs with a PCI-6111E acquisition card (National Instruments), and recorded to hard disk using the program Acquire (Buxton Corporation). Channel opening and closing transitions were determined using the program TAC 4.2.0 (Buxton Corporation), which digitally filters the data (Gaussian response, final effective bandwidth 5 kHz), interpolates the digitized points using a cubic spline function, and detects events using the half-amplitude threshold criterion, as

previously described (43). To determine single channel current amplitudes, the variable amplitude option in TAC was used, whereas to determine open and closed dwell times, the fixed amplitude option was used. Dwell time histograms were plotted using a logarithmic abscissa and square root ordinate (44), with a uniformly imposed dead time of 40 μ s, and fitted by the sum of exponentials by maximum likelihood using the program TACFit 4.2.0 (43). Clusters of channel

openings were identified as a series of closely spaced openings preceded and followed by closed intervals longer than a specified critical duration (τ_{crit}). This duration was taken as the point of intersection between consecutive components in the closed time histogram, and ranged between 1 and 30 ms. Cluster duration therefore comprises the total time of a series of openings plus that of the intervening closings briefer than τ_{crit} .

Acknowledgments: This work was supported in part by National Institutes of Health grant NS031744 to S. M. Sine.

Conflict of interest: The authors declare that they have no conflicts of interest with the contents of this article.

Author contributions: SS, SM and IB conceived and coordinated the study. SS and SM wrote the paper. SM performed patch-clamp experiments. SM and SS analyzed the results. All authors approved the final version of the manuscript.

REFERENCES

1. Millar, N. S., and Gotti, C. (2009) Diversity of vertebrate nicotinic acetylcholine receptors. *Neuropharmacology*. **56**, 237–46
2. Albuquerque, E. X., Pereira, E. F. R., Alkondon, M., and Rogers, S. W. (2009) Mammalian nicotinic acetylcholine receptors: from structure to function. *Physiol. Rev.* **89**, 73–120
3. Marubio, L. M., del Mar Arroyo-Jimenez, M., Cordero-Erausquin, M., Léna, C., Le Novère, N., de Kerchove d'Exaerde, A., Huchet, M., Damaj, M. I., and Changeux, J. P. (1999) Reduced antinociception in mice lacking neuronal nicotinic receptor subunits. *Nature*. **398**, 805–10
4. Picciotto, M. R., Zoli, M., Léna, C., Bessis, A., Lallemand, Y., Le Novère, N., Vincent, P., Pich, E. M., Brûlet, P., and Changeux, J. P. (1995) Abnormal avoidance learning in mice lacking functional high-affinity nicotine receptor in the brain. *Nature*. **374**, 65–7
5. Ross, S. A., Wong, J. Y., Clifford, J. J., Kinsella, A., Massalas, J. S., Horne, M. K., Scheffer, I. E., Kola, I., Waddington, J. L., Berkovic, S. F., and Drago, J. (2000) Phenotypic characterization of an alpha 4 neuronal nicotinic acetylcholine receptor subunit knock-out mouse. *J. Neurosci.* **20**, 6431–41
6. Zoli, M., Léna, C., Picciotto, M. R., and Changeux, J. P. (1998) Identification of four classes of brain nicotinic receptors using beta2 mutant mice. *J. Neurosci.* **18**, 4461–72
7. Zwart, R., and Vijverberg, H. P. (1998) Four pharmacologically distinct subtypes of alpha4beta2 nicotinic acetylcholine receptor expressed in *Xenopus laevis* oocytes. *Mol. Pharmacol.* **54**, 1124–31
8. Moroni, M., Zwart, R., Sher, E., Cassels, B. K., and Bermudez, I. (2006) alpha4beta2 nicotinic receptors with high and low acetylcholine sensitivity: pharmacology, stoichiometry, and sensitivity to long-term exposure to nicotine. *Mol. Pharmacol.* **70**, 755–68
9. Nelson, M. E., Kuryatov, A., Choi, C. H., Zhou, Y., and Lindstrom, J. (2003) Alternate stoichiometries of alpha4beta2 nicotinic acetylcholine receptors. *Mol. Pharmacol.* **63**, 332–41

10. Moroni, M., Vijayan, R., Carbone, A., Zwart, R., Biggin, P. C., and Bermudez, I. (2008) Non-agonist-binding subunit interfaces confer distinct functional signatures to the alternate stoichiometries of the $\alpha 4\beta 2$ nicotinic receptor: an $\alpha 4$ - $\alpha 4$ interface is required for Zn^{2+} potentiation. *J. Neurosci.* **28**, 6884–94
11. Timmermann, D. B., Sandager-Nielsen, K., Dyhring, T., Smith, M., Jacobsen, A.-M., Nielsen, E. Ø., Grunnet, M., Christensen, J. K., Peters, D., Kohlhaas, K., Olsen, G. M., and Ahring, P. K. (2012) Augmentation of cognitive function by NS9283, a stoichiometry-dependent positive allosteric modulator of $\alpha 2$ - and $\alpha 4$ -containing nicotinic acetylcholine receptors. *Br. J. Pharmacol.* **167**, 164–82
12. Tapia, L., Kuryatov, A., and Lindstrom, J. (2007) Ca^{2+} permeability of the $(\alpha 4)_3(\beta 2)_2$ stoichiometry greatly exceeds that of $(\alpha 4)_2(\beta 2)_3$ human acetylcholine receptors. *Mol. Pharmacol.* **71**, 769–76
13. Benallegue, N., Mazzaferro, S., Alcaino, C., and Bermudez, I. (2013) The additional ACh binding site at the $\alpha 4(+)/\alpha 4(-)$ interface of the $(\alpha 4\beta 2)_2 \alpha 4$ nicotinic ACh receptor contributes to desensitization. *Br. J. Pharmacol.* **170**, 304–16
14. Mazzaferro, S., Gasparri, F., New, K., Alcaino, C., Faundez, M., Iturriaga Vasquez, P., Vijayan, R., Biggin, P. C., and Bermudez, I. (2014) Non-equivalent ligand selectivity of agonist sites in $(\alpha 4\beta 2)_2 \alpha 4$ nicotinic acetylcholine receptors: a key determinant of agonist efficacy. *J. Biol. Chem.* **289**, 21795–806
15. Mazzaferro, S., Benallegue, N., Carbone, A., Gasparri, F., Vijayan, R., Biggin, P. C., Moroni, M., and Bermudez, I. (2011) Additional acetylcholine (ACh) binding site at $\alpha 4/\alpha 4$ interface of $(\alpha 4\beta 2)_2 \alpha 4$ nicotinic receptor influences agonist sensitivity. *J. Biol. Chem.* **286**, 31043–54
16. Harpsøe, K., Ahring, P. K., Christensen, J. K., Jensen, M. L., Peters, D., and Balle, T. (2011) Unraveling the high- and low-sensitivity agonist responses of nicotinic acetylcholine receptors. *J. Neurosci.* **31**, 10759–66
17. Lucero, L. M., Weltzin, M. M., Eaton, J. B., Cooper, J. F., Lindstrom, J. M., Lukas, R. J., and Whiteaker, P. (2016) Differential $\alpha 4(+)/(-)\beta 2$ agonist-binding site contributions to $\alpha 4\beta 2$ nicotinic acetylcholine receptor function within and between isoforms. *J. Biol. Chem.* **291**, 2444–2459
18. Carbone, a-L., Moroni, M., Groot-Kormelink, P.-J., and Bermudez, I. (2009) Pentameric concatenated $(\alpha 4)_2(\beta 2)_3$ and $(\alpha 4)_3(\beta 2)_2$ nicotinic acetylcholine receptors: subunit arrangement determines functional expression. *Br. J. Pharmacol.* **156**, 970–81
19. Zwart, R., Carbone, A. L., Moroni, M., Bermudez, I., Mogg, A. J., Folly, E. A., Broad, L. M., Williams, A. C., Zhang, D., Ding, C., Heinz, B. A., and Sher, E. (2008) Sazetidine-A is a potent and selective agonist at native and recombinant $\alpha 4 \beta 2$ nicotinic acetylcholine receptors. *Mol. Pharmacol.* **73**, 1838–43
20. Carignano, C., Barila, E. P., and Spitzmaul, G. (2016) Analysis of neuronal nicotinic acetylcholine receptor $\alpha 4\beta 2$ activation at the single-channel level. *Biochim. Biophys. Acta.* **1858**, 1964–73
21. Chen, Y., Sharples, T. J. W., Phillips, K. G., Benedetti, G., Broad, L. M., Zwart, R., and Sher, E. (2003) The nicotinic $\alpha 4\beta 2$ receptor selective agonist, TC-2559, increases dopamine neuronal activity in the ventral tegmental area of rat midbrain slices. *Neuropharmacology.* **45**, 334–344
22. Ragozzino, D., Fucile, S., Giovannelli, A., Grassi, F., Mileo, A. M., Ballivet, M., Alemà, S., and Eusebi, F. (1997) Functional properties of neuronal nicotinic acetylcholine receptor channels expressed in transfected human cells. *Eur. J. Neurosci.* **9**, 480–8
23. Ibañez-Tallon, I., Miwa, J. M., Wang, H.-L., Adams, N. C., Crabtree, G. W., Sine, S. M., and Heintz, N. (2002) Novel Modulation of Neuronal Nicotinic Acetylcholine Receptors by Association with the Endogenous Prototoxin lynx1. *Neuron.* **33**, 893–903

24. Hansen, S. B., Wang, H.-L., Taylor, P., and Sine, S. M. (2008) An ion selectivity filter in the extracellular domain of Cys-loop receptors reveals determinants for ion conductance. *J. Biol. Chem.* **283**, 36066–70
25. Imoto, K., Busch, C., Sakmann, B., Mishina, M., Konno, T., Nakai, J., Bujo, H., Mori, Y., Fukuda, K., and Numa, S. (1988) Rings of negatively charged amino acids determine the acetylcholine receptor channel conductance. *Nature.* **335**, 645–8
26. Mukhtasimova, N., Lee, W. Y., Wang, H.-L., and Sine, S. M. (2009) Detection and trapping of intermediate states priming nicotinic receptor channel opening. *Nature.* **459**, 451–4
27. Lape, R., Colquhoun, D., and Sivilotti, L. G. (2008) On the nature of partial agonism in the nicotinic receptor superfamily. *Nature.* **454**, 722–7
28. Sakmann, B., Patlak, J., and Neher, E. (1980) Single acetylcholine-activated channels show burst-kinetics in presence of desensitizing concentrations of agonist. *Nature.* **286**, 71–3
29. Olsen, J. A., Kastrup, J. S., Peters, D., Gajhede, M., Balle, T., and Ahring, P. K. (2013) Two distinct allosteric binding sites at $\alpha 4\beta 2$ nicotinic acetylcholine receptors revealed by NS206 and NS9283 give unique insights to binding activity-associated linkage at Cys-loop receptors. *J. Biol. Chem.* **288**, 35997–6006
30. Unwin, N. (2005) Refined structure of the nicotinic acetylcholine receptor at 4Å resolution. *J. Mol. Biol.* **346**, 967–89
31. Morales-Perez, C. L., Noviello, C. M., and Hibbs, R. E. (2016) X-ray structure of the human $\alpha 4\beta 2$ nicotinic receptor. *Nature.* **538**, 411–415
32. Jeanclos, E. M., Lin, L., Treuil, M. W., Rao, J., DeCoster, M. A., and Anand, R. (2001) The Chaperone Protein 14-3-3 η Interacts with the Nicotinic Acetylcholine Receptor $\alpha 4$ Subunit. *J. Biol. Chem.* **276**, 28281–28290
33. Pear, W. S., Nolan, G. P., Scott, M. L., and Baltimore, D. (1993) Production of high-titer helper-free retroviruses by transient transfection. *Proc. Natl. Acad. Sci. U. S. A.* **90**, 8392–6
34. Sine, S. M. (1993) Molecular dissection of subunit interfaces in the acetylcholine receptor: identification of residues that determine curare selectivity. *Proc. Natl. Acad. Sci. U. S. A.* **90**, 9436–40
35. Sine, S. M., Quiram, P., Papanikolaou, F., Kreienkamp, H. J., and Taylor, P. (1994) Conserved tyrosines in the alpha subunit of the nicotinic acetylcholine receptor stabilize quaternary ammonium groups of agonists and curariform antagonists. *J. Biol. Chem.* **269**, 8808–16
36. Bouzat, C., Bren, N., and Sine, S. M. (1994) Structural basis of the different gating kinetics of fetal and adult acetylcholine receptors. *Neuron.* **13**, 1395–402
37. Cooper, S. T., Harkness, P. C., Baker, E. R., and Millar, N. S. (1999) Up-regulation of cell-surface $\alpha 4\beta 2$ neuronal nicotinic receptors by lower temperature and expression of chimeric subunits. *J. Biol. Chem.* **274**, 27145–27152
38. Hamill, O. P., Marty, A., Neher, E., Sakmann, B., and Sigworth, F. J. (1981) Improved patch-clamp techniques for high-resolution current recording from cells and cell-free membrane patches. *Pflügers Arch. Eur. J. Physiol.* **391**, 85–100
39. Rayes, D., Spitzmaul, G., Sine, S. M., and Bouzat, C. (2005) Single-channel kinetic analysis of chimeric $\alpha 7$ -5HT3A receptors. *Mol. Pharmacol.* **68**, 1475–83
40. Bouzat, C., Bartos, M., Corradi, J., and Sine, S. M. (2008) The interface between extracellular and transmembrane domains of homomeric Cys-loop receptors governs open-channel lifetime and rate of desensitization. *J. Neurosci.* **28**, 7808–19
41. Sine, S. M., Claudio, T., and Sigworth, F. J. (1990) Activation of Torpedo acetylcholine receptors expressed in mouse fibroblasts. Single channel current kinetics reveal distinct agonist binding affinities. *J. Gen. Physiol.* **96**, 395–437

42. Mukhtasimova, N., daCosta, C. J. B., and Sine, S. M. (2016) Improved resolution of single channel dwell times reveals mechanisms of binding, priming, and gating in muscle AChR. *J. Gen. Physiol.* **148**, 43–63
43. Colquhoun, D., and Sigworth, F. L. (1983) Fitting and statistical analysis of single channel records. in *In Single Channel Recording*, pp. 483–587, Springer US, Boston, MA, 10.1007/978-1-4615-7858-1_11
44. Sigworth, F. J., and Sine, S. M. (1987) Data transformations for improved display and fitting of single-channel dwell time histograms. *Biophys. J.* **52**, 1047–54

Table 1- *Open durations of unlinked and linked receptors activated by ACh.* Mean open times (O) in units of milliseconds and fractional areas (A) are given along with the standard error (\pm SEM) for the indicated number of patches, n. In cases in which SEM is not given, the frequency of channel openings in individual patches was low and the indicated number of patches was combined prior to fitting.

| | O1 (A1) | O2 (A2) | O3 (A3) | O4 (A4) |
|--|---------------------------------------|--------------------------------------|--------------------------------------|-------------------------------------|
| Unlinked $\alpha 4:\beta 2$ 1:10 n=3 | 0.023 \pm 0.01 (0.36 \pm 0.09) | 0.28 \pm 0.02 (0.39 \pm 0.13) | 1.36 \pm 0.21 (0.19 \pm 0.07) | 6.6 \pm 2.02 (0.06 \pm 0.04) |
| Linked $(\alpha 4\beta 2)_2\beta 2$ n=3 | 0.047 (0.17) | 0.34 (0.53) | 0.85 (0.25) | 6.6 (0.05) |
| Unlinked $\alpha 4:\beta 2$ 10:1 n=4 | 0.063 \pm 0.04 (0.64 \pm 0.04) | 0.21 \pm 0.23 (0.31 \pm 0.05) | 1.5 \pm 0.54 (0.05 \pm 0.01) | |
| Linked $(\alpha 4\beta 2)_2\alpha 4$ n=3 | 0.18 (0.31) | 1.49 (0.44) | 3.9 (0.25) | |

Table 2- *Open durations of unlinked and linked receptors activated by ACh \pm NS-9283.* Mean open times (O) in units of milliseconds and fractional areas (A) are given along with the standard error (\pm SEM) for the indicated number of patches, n. In cases in which SEM is not given, the frequency of channel openings in individual patches was low and the indicated number of patches was combined prior to fitting.

| | | O1 (A1) | O2 (A2) | O3 (A3) | O4 (A4) |
|---|-------------------------|---|--|--|-------------------------------------|
| Unlinked $\alpha 4:\beta 2$ 1:10 | ACh n=2 | 0.022 (0.42) | 0.26 (0.28) | 1.6 (0.24) | 8.6 (0.06) |
| | ACh + NS-9283 n=2 | 0.016 \pm 0.019 (0.38 \pm 0.02) | 0.15 \pm 0.06 (0.21 \pm 0.06) | 0.7 \pm 0.1 (0.37 \pm 0.17) | 2 \pm 0.3 (0.04 \pm 0.01) |
| Linked ($\alpha 4\beta 2$)₂$\beta 2$ | ACh n=4 | 0.065 (0.21) | 0.43 (0.66) | 1.5 (0.10) | 8 (0.03) |
| | ACh + NS-9283 n=3 | 0.035 (0.32) | 0.27 (0.44) | 0.70 (0.24) | 3.4 (0.01) |
| Unlinked $\alpha 4:\beta 2$ 10:1 | ACh n=3 | 0.070 \pm 0.006 (0.34 \pm 0.02) | 0.62 \pm 0.05 (0.58 \pm 0.002) | 2.2 \pm 0.2 (0.08 \pm 0.017) | |
| | ACh + NS-9283 n=3 | 0.029 \pm 0.002 (0.40 \pm 0.04) | 0.28 \pm 0.03 (0.41 \pm 0.05) | 1.02 \pm 0.15 (0.19 \pm 0.013) | |
| Linked ($\alpha 4\beta 2$)₂$\alpha 4$ | ACh n=5 | 0.029 (0.15) | 0.34 (0.71) | 1.7 (0.15) | |
| | ACh + NS-9283 n=3 | 0.030 \pm 0.001 (0.36 \pm 0.11) | 0.37 \pm 0.05 (0.52 \pm 0.04) | 1.38 \pm 0.6 (0.12 \pm 0.07) | |

Table 3- Cluster durations of unlinked and linked receptors activated by ACh \pm NS-9283. Mean cluster durations (Cd) in units of milliseconds and fractional areas (A) are given along with \pm SEM for the indicated number of patches, n. In cases in which SEM is not given, the frequency of channel openings in individual patches was low and the indicated number of patches was combined prior to fitting.

| | | Cd1 (A1) | Cd2 (A2) | Cd3 (A3) | Cd4 (A4) | Cd5 (A5) |
|---|--|--|---|--|--|----------------|
| Unlinked $\alpha 4:\beta 2$ 1:10 | ACh n=2 | 0.034 (0.38) | 0.38 (0.32) | 1.2 (0.19) | 5.4 (0.08) | 21.7 (0.03) |
| | ACh + NS-9283 n=2; $\tau_{crit}=1$ ms | 0.067 \pm 0.03 (0.20 \pm 0.03) | 0.58 \pm 0.009 (0.53 \pm 0.2) | 2.4 \pm 0.6 (0.27 \pm 0.18) | | |
| Linked ($\alpha 4\beta 2$)₂$\beta 2$ | ACh n=4; $\tau_{crit}=1$ ms | 0.028 (0.20) | 0.33 (0.48) | 1.1 (0.30) | 22 (0.2) | |
| | ACh + NS-9283 n=2; $\tau_{crit}=1$ ms | 0.038 (0.32) | 0.28 (0.40) | 0.76 (0.27) | 5 (0.01) | |
| Unlinked $\alpha 4:\beta 2$ 10:1 | ACh n=3; $\tau_{crit}=1$ ms | 0.048 \pm 0.012 (0.31 \pm 0.16) | 0.55 \pm 0.11 (0.53 \pm 0.06) | 2.4 \pm 0.3 (0.16 \pm 0.07) | | |
| | ACh + NS-9283 n=3; $\tau_{crit}=30$ ms | 0.02 \pm 0.003 (0.43 \pm 0.12) | 0.25 \pm 0.06 (0.17 \pm 0.014) | 1.57 \pm 0.09 (0.22 \pm 0.05) | 16.7 \pm 0.25 (0.18 \pm 0.05) | |
| Linked ($\alpha 4\beta 2$)₂$\alpha 4$ | ACh n=5 $\tau_{crit}=1$ ms | 0.28 (0.17) | 0.37 (0.71) | 2.5 (0.13) | | |
| | ACh + NS-9283 n=3; $\tau_{crit}=10$ ms | 0.036 (0.39) | 0.755 (0.34) | 10 (0.26) | | |

Table 4- Summary of Stoichiometry-Dependent Properties

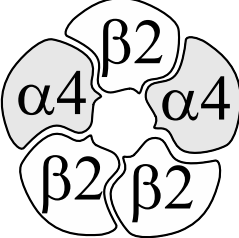
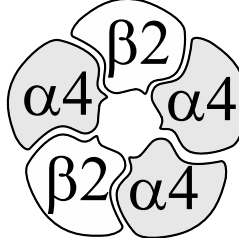
| Attribute | $(\alpha 4\beta 2)_2\beta 2$  | $(\alpha 4\beta 2)_2\alpha 4$  |
|-------------------------------------|---|--|
| Number of agonist binding sites | 2 | 3 |
| Binding site symmetry | Asymmetric | Asymmetric |
| Expected number of occupancy states | 3 (1, 1, 2) | 7 (1, 1, 1, 2, 2, 2, 3) |
| Observed number of open states | 4 | 3 |
| Net charge of external ring | + 1 | - 1 |
| Unitary conductance | 48 pS | 60 pS |
| Potentiation by NS-9283 | No | Yes |

FIGURE LEGENDS

FIGURE 1. *Identification of single channel currents from $\alpha 4\beta 2$ nAChRs.* BOSC 23 cells were transfected with (A) unlinked (1:1 ratio) or (B) linked subunit cDNAs. A cell-attached patch was established with a patch pipette containing agonist-free pipette solution, a holding potential of -70 mV was applied, and current was recorded before and after adding nicotine (thick bar) to the bathing solution. In each panel, the traces show nicotine-induced single channel currents (upward deflections, 3 kHz Gaussian filter) at compressed and expanded time scales. For unlinked subunits, all-points amplitude histograms from two regions of the recording are superimposed, revealing amplitudes of 3.2 ± 0.4 and 4.1 ± 0.5 pA (A), whereas for linked subunits, a representative histogram from one region shows an amplitude of 4.3 ± 0.5 pA. Amplitudes are expressed as the mean \pm SD.

FIGURE 2. *Deducing the stoichiometry of $\alpha 4$ and $\beta 2$ subunits based on unitary current amplitude.* BOSC 23 cells were transfected with unlinked (A-C) or linked (D-E) subunit cDNAs. Single channel currents were recorded in the cell-attached patch configuration with a concentration of 10 μ M ACh in the pipette and a holding potential of -70 mV. Next to each trace is a histogram of detected single channel currents that reached full amplitude with the indicated means and SD of each Gaussian peak. Panel F plots unitary current against holding potential for the indicated receptors with the slope of each fitted line giving the single channel conductance. Panel G shows results using the $\alpha 4\beta 2$ selective agonist TC-2559 for the indicated receptors; histograms of detected single channel currents that reached full amplitude are shown with the indicated means and SD of the fitted Gaussian peak.

FIGURE 3. *Dependence of open channel lifetime on subunit stoichiometry.* BOSC 23 cells were transfected with unlinked (A, C) or linked (B, D) subunit cDNAs. Single channel currents were recorded in the cell-attached patch configuration with a concentration of 10 μ M ACh in the pipette and a holding potential of -70 mV. For each panel, single channel currents are displayed at a bandwidth of 5 kHz, and the corresponding open duration histogram is displayed with the fit of sums of exponentials superimposed. Fitted parameters are listed in Table 1. For each panel, a histogram of detected single channel currents that reached full amplitude is shown along with a representative trace filtered at 2 kHz.

FIGURE 4. *NS-9283 potentiates high conductance receptors with three $\alpha 4$ and two $\beta 2$ subunits.* BOSC 23 cells were transfected with the indicated unlinked (A, B) or linked (C, D) subunit cDNAs. Single channel currents were recorded in the cell-attached patch configuration with a concentration of 10 μ M ACh in the pipette, without or with 10 μ M NS-9283, and a holding potential of -70 mV. For each panel, single channel currents at a bandwidth of 3 kHz are shown, along with closed, open and cluster duration histograms fitted by sums of exponentials. The critical time, τ_{crit} , for generating cluster duration histograms is indicated by the arrow. Fitted parameters are listed in Tables 2 and 3.

FIGURE 5. *Increase in the number of channel reopenings per cluster by NS-9283 for receptors with three $\alpha 4$ and two $\beta 2$ subunits.* BOSC 23 cells were transfected with the indicated unlinked (A) or linked (B) subunit cDNAs as in Fig. 4. The fraction of clusters with more than a given number of channel reopenings was determined from 3 to 5 recordings for each condition and plotted along with S.E.M. For recordings in the presence of ACh alone, a single exponential is fitted to the distributions. For unlinked subunits, the mean number of reopenings per cluster, $\tau=0.55 \pm 0.007$, while that for linked subunits, $\tau=0.43 \pm 0.04$. For recordings in the presence of ACh and NS-9283, the sum of two exponentials is fitted to the distributions. For unlinked

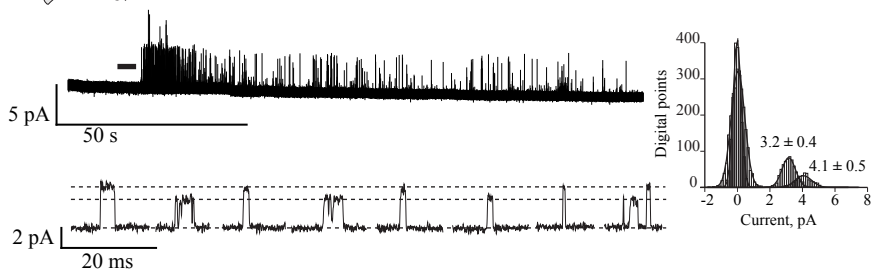
subunits, the mean number of reopenings per cluster and fractional area are, $\tau_1 = 1.16 \pm 0.07$, $a_1 = 0.68 \pm 0.055$, and $\tau_2 = 3.5 \pm 0.29$, $a_2 = 0.32$, while for linked subunits, $\tau_1 = 1.12 \pm 0.13$, $a_1 = 0.73 \pm 0.04$, and $\tau_2 = 9.94 \pm 1.6$, $a_2 = 0.27$.

FIGURE 6. *NS-9283 does not potentiate low conductance receptors with two $\alpha 4$ and three $\beta 2$ subunits.* BOSC 23 cells were transfected with the indicated unlinked (A, B) or linked (C, D) subunit cDNAs. Single channel currents were recorded in the cell-attached patch configuration with a concentration of 10 μM ACh in the pipette, without or with 10 μM NS-9283, and a holding potential of -70 mV, as in Fig. 4. For each panel, closed, open and cluster duration histograms, fitted by sums of exponentials, are shown. The critical time, τ_{crit} , for generating cluster duration histograms is indicated by the arrow. Fitted parameters are listed in Tables 2 and 3.

Figure 1

A

$\alpha 4 + \beta 2$



B

$\beta 2$
 $\alpha 4$ $\alpha 4$
 $\beta 2$ $\alpha 4$

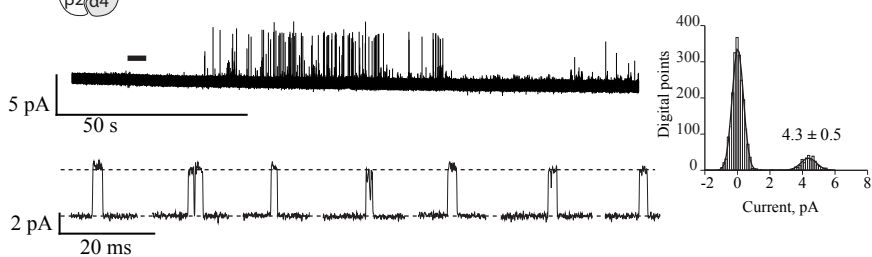


Figure 2

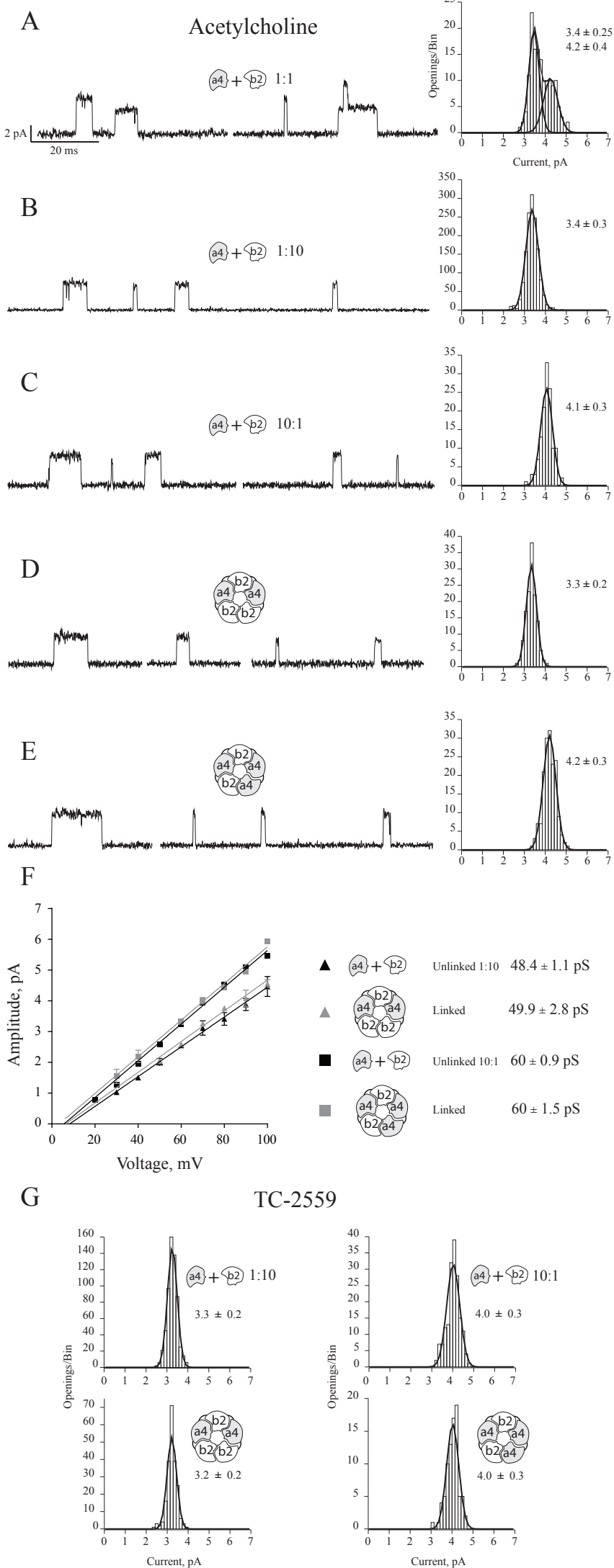
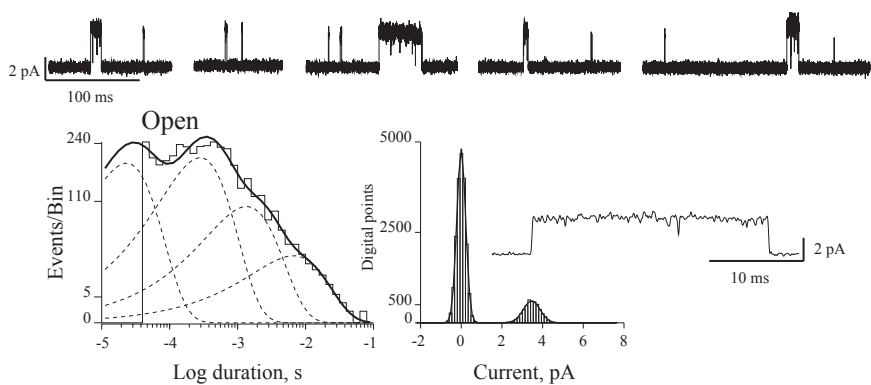
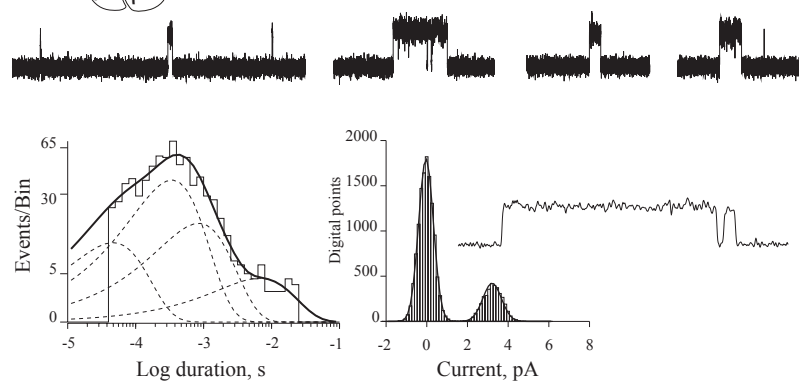


Figure 3

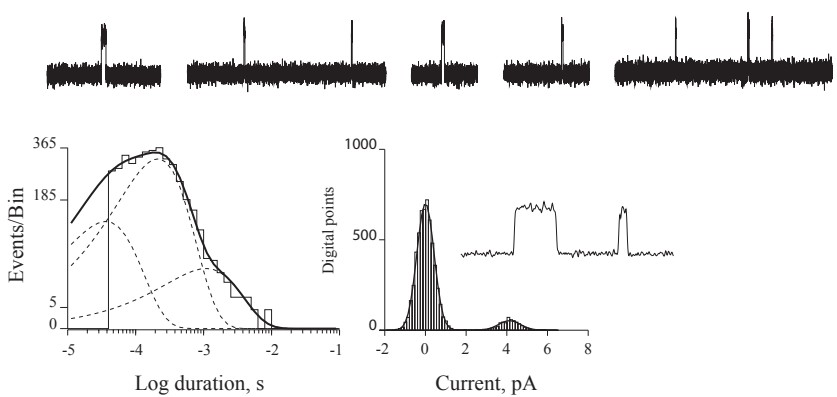
A $\alpha 4 + \beta 2$ 1:10 Low conductance



B $\alpha 4 + \beta 2$ 1:10 High conductance



C $\alpha 4 + \beta 2$ 10:1 High conductance



D $\alpha 4 + \beta 2$ 10:1 Low conductance

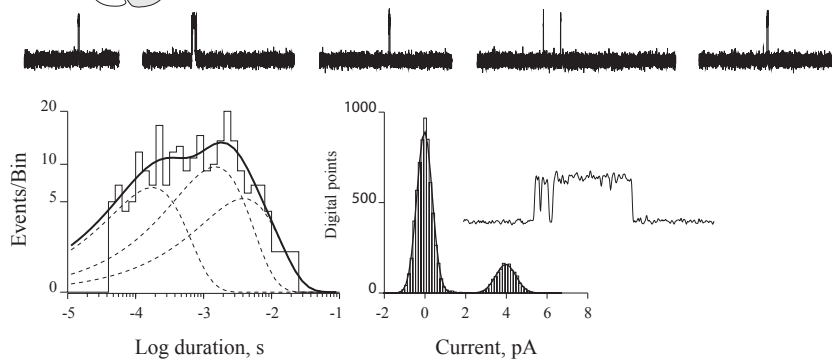
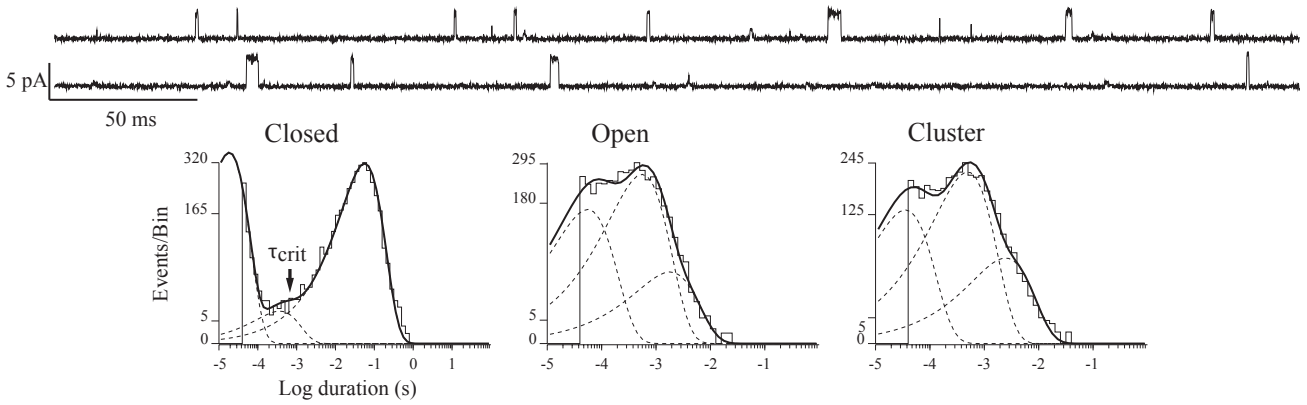


Figure 4

A

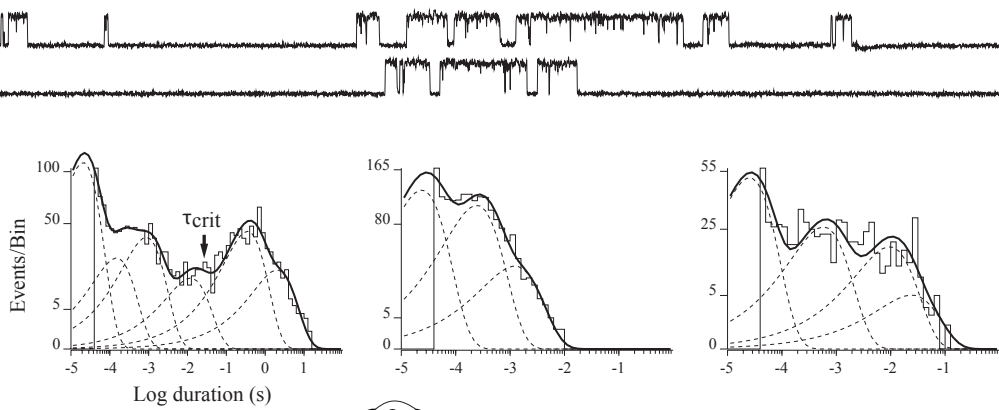
ACh 10 μ M

$\alpha 4 + \beta 2$ High conductance



B

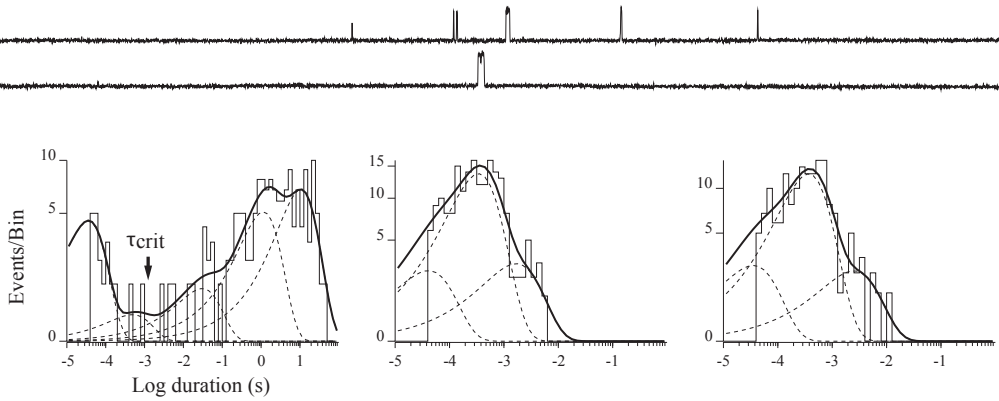
ACh 10 μ M + NS-9283 10 μ M



C

ACh 10 μ M

$\beta 2 + \alpha 4$ High conductance



D

ACh 10 μ M + NS-9283 10 μ M

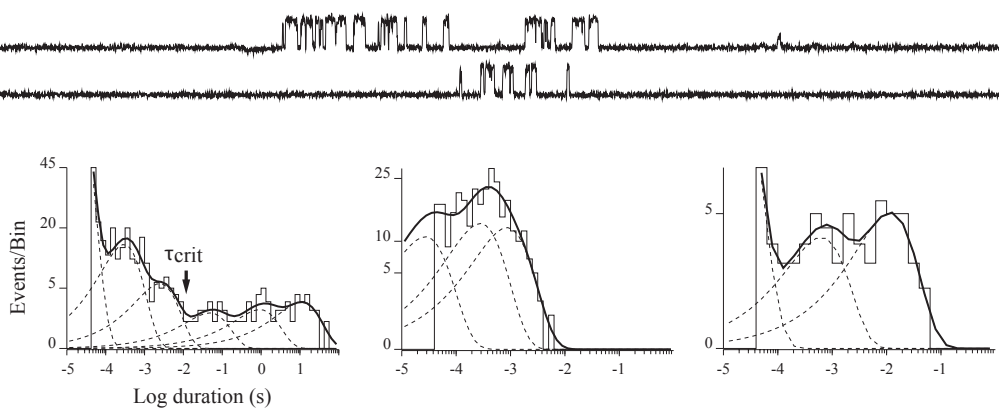
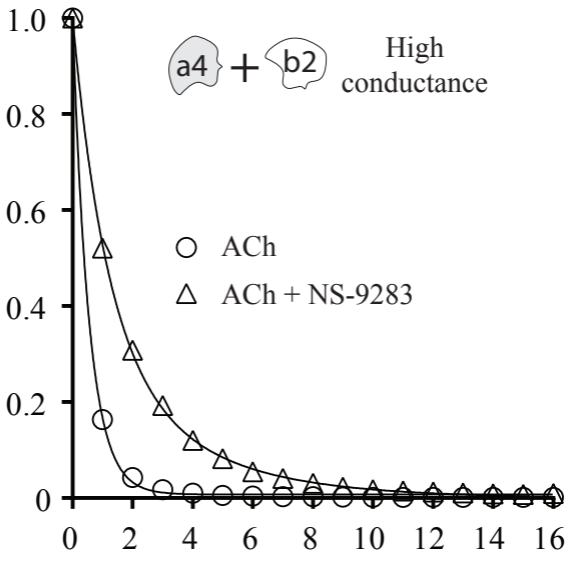


Figure 5

A



B

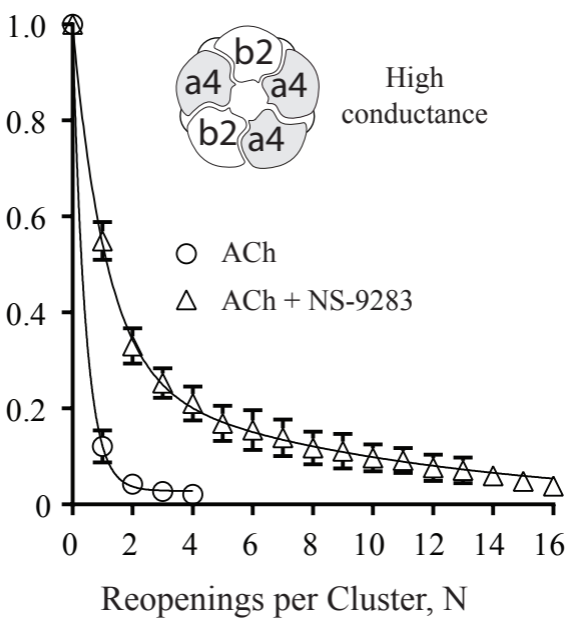
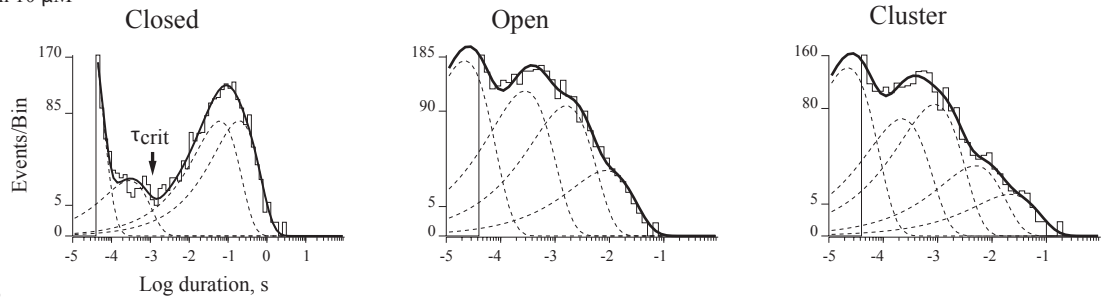


Figure 6

$\alpha 4 + \beta 2$ Low conductance

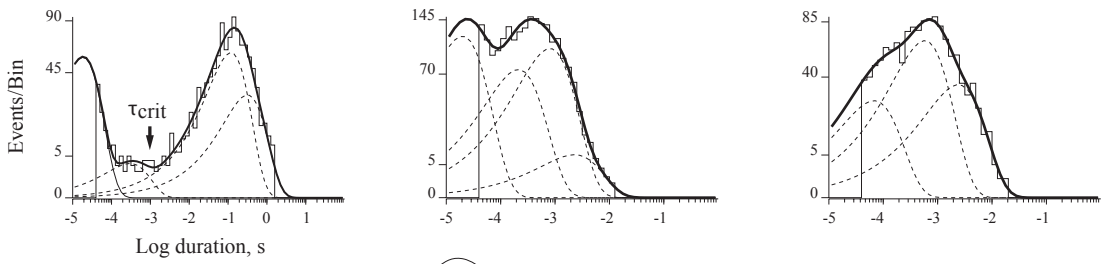
A

ACh 10 μ M



B

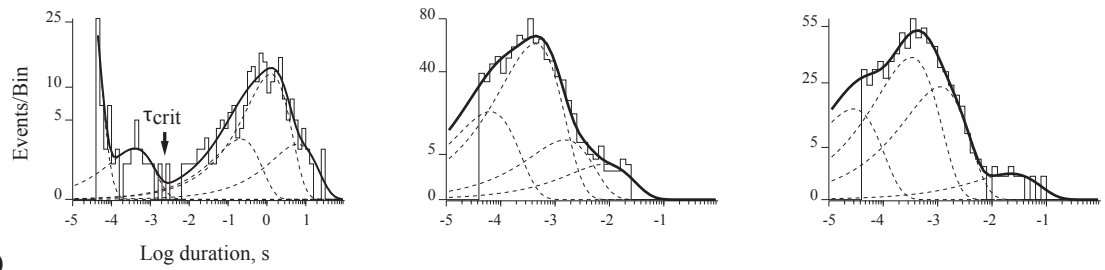
ACh 10 μ M + NS-9283 10 μ M



C

ACh 10 μ M

$\alpha 4 \beta 2$
 $\beta 2 \alpha 4$
 $\beta 2 \beta 2$ Low conductance



D

ACh 10 μ M + NS-9283 10 μ M

